

BULLETIN OF THE CHEMICAL SOCIETY OF JAPAN, VOL. 46, 1329—1333 (1973)

**Semiconducting Properties of  $\text{Ln}_2\text{CuO}_4$  (Ln=Rare earths)**

Tadao KENJO and Seishi YAJIMA

*The Oarai Branch, The Research Institute for Iron, Steel and Other Metals,  
Tohoku University, Oarai, Ibaraki-ken*

(Received July 19, 1972)

The temperature dependence of the resistivity and the thermoelectric power of  $\text{Ln}_2\text{CuO}_4$  (Ln=rare earths) have been measured. The compounds of Gd, Sm, Nd, and Pr are semiconductive, while  $\text{La}_2\text{CuO}_4$  shows metallic conductivity. The tetragonal lattice of  $\text{La}_2\text{CuO}_4$  shrinks in the *a* axis and expands in the *c* axis compared to  $\text{Pr}_2\text{CuO}_4$ , in spite of the steady expansion of these lattice parameters for the compounds between Gd and Pr. The thermoelectric power of  $\text{Ln}_2\text{CuO}_4$ , but not  $\text{La}_2\text{CuO}_4$ , is negative, suggesting an electron-conducting or *n*-type semiconductor. The resistivity of the  $\text{Ln}_2\text{CuO}_4$  at room temperature increases essentially with an increase in the atomic number of Ln. The plots of the thermoelectric power *vs.* the reciprocal temperature showed a steeper slope for the compounds of the heavier rare earths. The semiconductor-metal transition observed between  $\text{La}_2\text{CuO}_4$  and  $\text{Pr}_2\text{CuO}_4$  was explained in relation to the structural change (the shrinkage of the *a* axis and the expansion of the *c* axis) as being due to the change in the electron configurations of  $\text{Cu}^{2+}$ .

In the rare earth oxide-cupric oxide system, two different compounds were found:  $\text{Ln}_2\text{CuO}_4$  (Ln=La, Pr, Nd, Sm, and Gd)<sup>1)</sup> and  $\text{Ln}_2\text{Cu}_2\text{O}_5$  (Ln=Tb, Dy, Er, Yb, and Y).<sup>2)</sup> Tm, Ho, and Lu were expected to be of the same type as the latter one.<sup>2)</sup> The  $\text{Ln}_2\text{CuO}_4$  compounds are isostructural with tetragonal  $\text{K}_2\text{NiF}_4$ , whose space group is  $D_{4h}^{17}$  ( $I4/mmm$ ).<sup>3)</sup>

It should be noted that  $\text{Ln}_2\text{CuO}_4$  is black.<sup>1)</sup> The black color suggests that an appreciable number of electrons in the valence state are excited to a higher

energy level by thermal energy as low as room temperature. Therefore, if the higher energy level to which electrons are excited is a conduction band, the conductivity of  $\text{Ln}_2\text{CuO}_4$  will be in the region of the semiconductor. Further, the crystal structure of  $\text{Ln}_2\text{CuO}_4$  seems to support the above expectation. In the crystal lattice of  $\text{Ln}_2\text{CuO}_4$ ,  $\text{Cu}^{2+}$  is surrounded by six  $\text{O}^{2-}$  ions and forms a Cu-O-Cu chain toward the *a* axis without an interruption by  $\text{Ln}^{3+}$ . Since 3d-transition metals are thought to make an electron overlapping with  $\text{O}^{2-}$ ,<sup>4-6)</sup> and since, in fact, the conductivity of

1) R. H. Frushour and K. S. Vorres, AEC Rept. TID-2207 Page E. 1965.

2) O. Schmitz-DuMont and H. Kasper, *Monatsh. Chem.*, **96**, 506 (1965).

3) R. W. G. Wyckoff, "Crystal Structures," Vol. 3, Interscience Publishers, New York, N.Y. (1965), p. 68.

4) C. N. R. Rao and G. V. Subba Rao, *Phys. Stat. Sol. (a)*, **1**, 597 (1970).

5) P. M. Raccach and J. B. Goodenough, *J. Appl. Phys.*, **39**, 1209 (1968).

6) J. B. Goodenough, *Phys. Rev.*, **164**, 785 (1967).

many oxides containing 3d-transition metals is in the region of the semiconductor,<sup>4-6)</sup> it is very likely that the Cu-O-Cu chain in the  $\text{Ln}_2\text{CuO}_4$  can be a path for electron transfer.

On the other hand, the role of  $\text{Ln}^{3+}$  in electrical conduction may not be as important as that of  $\text{Cu}^{2+}$ , because in the Ln-O bond such an electron overlapping as would contribute to electrical conduction cannot be expected. However,  $\text{Ln}^{3+}$  may affect the electrical properties and the structure of the compounds indirectly. The configuration of electrons of  $\text{Cu}^{2+}$ , particularly those of 3d-electrons, are influenced by the ligand field caused mainly by the effective negative charges on the six  $\text{O}^{2-}$  surrounding  $\text{Cu}^{2+}$  ions. Since the less electronegative rare earth, or larger rare earth cation, pushes electrons more strongly toward oxygen in the Ln-O bond, the effective negative charges on the  $\text{O}^{2-}$  of the compounds of less electronegative rare earth can be expected to be greater; in other words, the ligand field at the site of  $\text{Cu}^{2+}$  is made stronger by replacing Ln with less electronegative Ln. At this time it is difficult to make more detailed predictions of the effect of the ligand-field strength changed by various rare earth cations on the electrical properties of the compounds, but it would be interesting to see if the  $\text{Ln}_2\text{-CuO}_4$  compounds show semiconducting properties and if their electrical conductivity depends upon the size of the rare earth cations.

From the above reason, the compounds of La, Pr, Nd, Sm, and Gd were prepared, and their semiconducting properties investigated.

## Experimental

**Material and Reagents.** Stock solutions of cupric nitrate were prepared by dissolving cupric nitrate of the Kanto Chemical Co., GR grade, into distilled water. Stock solutions of rare earth nitrates were prepared by dissolving each rare earth oxide (99.9% purity; Nippon Yttrium Co., Ltd.) into nitric acid. Both cupric nitrate and rare earth nitrate solutions were standardized against an EDTA standard solution, using XO as the indicator.

**Procedure.** The  $\text{Ln}_2\text{CuO}_4$  samples were prepared from gel-like mixed hydroxides. This method is advantageous in giving well-mixed oxide mixtures and denser final specimens than the usual ceramic technique which consists of heating a mixture of the oxides of Cu and Ln. Aliquot portions of cupric nitrate and rare earth nitrate solutions were mixed together, and then a 1 M-NaOH solution was stirred in at 80 °C. The final pH of the solution was adjusted to 11. After the mixture had stood overnight, the mixed precipitates of the hydroxides were filtered and repeatedly washed with distilled water until no sodium ion was detected in the filtrate by the flame test. The gel-like mixtures thus obtained were dried at 120 °C and preheated at 750 °C for 4 hr in air. The samples thus obtained, partially converted to  $\text{Ln}_2\text{CuO}_4$ , were milled, pressed into 15-mm $\phi$  pellets under a pressure of 2.5 t/cm<sup>2</sup>, and heated again at 1000 °C for 15 hr in air. Then they were removed from the furnace and cooled in air to room temperature. The mole ratio of Cu to Ln of the samples thus obtained was determined by the following chelatometric titration method. Two aliquot portions were taken from sample solutions obtained by dissolving sample specimens into nitric acid. The total content of  $\text{Cu}^{2+}$  and

$\text{Ln}^{3+}$  in the first sample solution was determined using PAN as the indicator. The solution of sodium thiosulfate was added to the second one in order to mask the  $\text{Cu}^{2+}$ , and then the  $\text{Ln}^{3+}$  was titrated, using XO as the indicator. The  $\text{Cu}^{2+}$  content was calculated from the difference between the two titration data. The results of the chemical analysis showed  $\text{Ln}_2\text{O}_3/\text{CuO}=1$  within  $\pm 0.5\%$  for all the samples obtained. The bulk densities of the specimens obtained were 90–95% of the theoretical values calculated from the X-ray diffraction data. All the samples were found to be single-phase by means of an X-ray diffractometer.

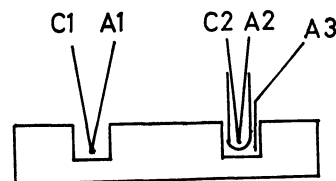


Fig. 1. A device for thermoelectric power measurements. C: chromel wire, A: alumel wire, C2-A2 thermocouple is coated with glass.

For the measurements of the resistivity and of the thermoelectric power, rods 12–13 mm long and 3–4 mm thick were used. The resistivity was measured by the 4-probe method, using Conductive Silver Coating Materials of Du Pont No. 6422 to connect the silver electrode with the oxide specimens. The thermoelectric power was measured using alumel-chromel thermocouples, as is shown in Fig. 1. Two couples of alumel-chromel thermocouples were inserted into two holes cut 8 mm apart in the specimen rods. One of them was coated with glass in order to avoid a short circuit through the rod (C2, A2),<sup>7)</sup> and an additional alumel wire was attached to the hole in which the glass-coated thermocouple had been inserted (A3). All the contact between the specimens and the thermocouple wires was made using the Conductive Silver Coating Materials of Du Pont No. 6422. Since this contacting procedure involves heating at 700 °C for 4 hr and subsequent gradual cooling, the sample ends in being annealed. The sample temperature was measured by means of a C1-A1 thermocouple. The temperature difference was taken up from the A1-A2 couple while the C1 was connected with the C2. The potential difference due to the thermoelectric power was measured from the A1-A3 couple. The temperature difference between the two holes was adjusted to be less than 5 °C. All the voltage measurements for resistivity and thermoelectric power were performed by means of a Hitachi QPD<sub>74</sub> potentiometric 2-pen recorder.

## Results

The temperature dependences of the resistivity of various  $\text{Ln}_2\text{CuO}_4$  are given in Fig. 2. Corrections for the bulk density were made by dividing the raw data by the ratio of the bulk to the theoretical density. These results indicate that the  $\text{Ln}_2\text{CuO}_4$  (Ln=Gd~Pr) compounds are semiconductive and that  $\text{La}_2\text{CuO}_4$  compound is metallic. The slopes in these plots are steeper in the higher temperature region than in the lower one except for metallic  $\text{La}_2\text{CuO}_4$ . These plots all seem to fall on identical curves in the high-temperature region.

7) The conductivity of the samples is so high, particularly at the high temperatures, that the temperature difference cannot be measured unless one of the thermocouples is glass-coated.

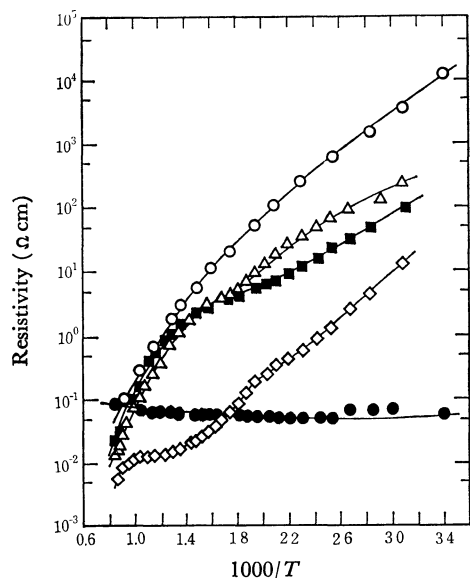


Fig. 2. Temperature dependence of resistivity of various  $\text{Ln}_2\text{CuO}_4$  compounds.

○:  $\text{Gd}_2\text{CuO}_4$ , △:  $\text{Nd}_2\text{CuO}_4$ , ■:  $\text{Sm}_2\text{CuO}_4$ ,  
◇:  $\text{Pr}_2\text{CuO}_4$ , ●:  $\text{La}_2\text{CuO}_4$ .

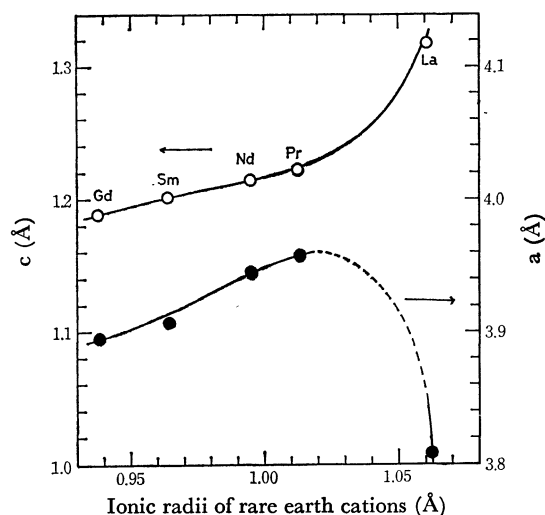


Fig. 3. Lattice parameters of various  $\text{Ln}_2\text{CuO}_4$  compounds.

○: c axis ●: a axis

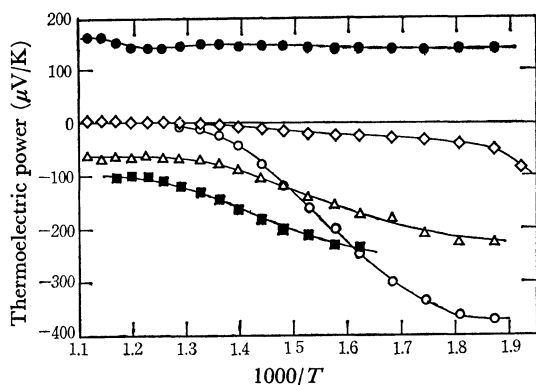


Fig. 4. Temperature dependence of thermoelectric power of various  $\text{Ln}_2\text{CuO}_4$  compounds.

○:  $\text{Gd}_2\text{CuO}_4$ , △:  $\text{Nd}_2\text{CuO}_4$ , ■:  $\text{Sm}_2\text{CuO}_4$ ,  
◇:  $\text{Pr}_2\text{CuO}_4$ , ●:  $\text{La}_2\text{CuO}_4$ .

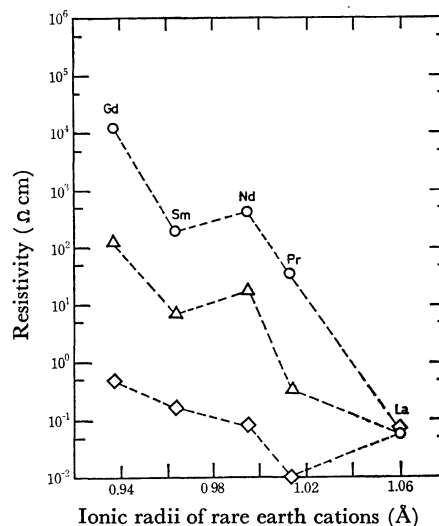


Fig. 5. Relation between resistivity and ionic radii of rare-earth cations of  $\text{Ln}_2\text{CuO}_4$  compounds.

○: room temperature, △: 200 °C, ◇: 800 °C

The semiconductor-metal transition observed between  $\text{Pr}_2\text{CuO}_4$  and  $\text{La}_2\text{CuO}_4$  corresponds to the structural behavior of  $\text{Ln}_2\text{CuO}_4$  shown in Fig. 3; the parameters of the tetragonal lattice,  $c$  and  $a$ , increase with an increase in the ionic radii of  $\text{Ln}^{3+}$  between Gd and Pr, but the  $c$  axis of  $\text{La}_2\text{CuO}_4$  expands more greatly than would be expected from the manner between Pr and Gd and its  $a$  axis shrinks by 3.8% against that of  $\text{Pr}_2\text{CuO}_4$ .

As can be seen in Fig. 4, the thermoelectric power,  $\alpha$ , in all the  $\text{Ln}_2\text{CuO}_4$  compounds except for  $\text{La}_2\text{CuO}_4$  is negative, suggesting an  $n$ -type semiconductor. The slopes in the  $\alpha$  vs.  $1/T$  plots decrease in this order,  $\text{Gd} < \text{Sm} \approx \text{Nd} < \text{Pr}$ .

Figure 5 shows a dependence of the resistivity on the ionic radii<sup>8)</sup> of the rare earth cations of  $\text{Ln}_2\text{CuO}_4$ . At room temperature, the resistivity decreases essentially with an increase in the ionic radii of rare earth cations and at high temperatures it is not so dependent on the ionic radii.

## Discussion

The experimental results of this work can be summarized as follows: (1) All the  $\text{Ln}_2\text{CuO}_4$  compounds except for  $\text{La}_2\text{CuO}_4$  are semiconductive, while  $\text{La}_2\text{CuO}_4$  is metallic. (2) The resistivity,  $\rho$ , of  $\text{Ln}_2\text{CuO}_4$  decreases essentially with an increase in the ionic radii of  $\text{Ln}^{3+}$ , most markedly at room temperature. The slopes of the  $\log \rho - 1/T$  plots of all the  $\text{Ln}_2\text{CuO}_4$  except for  $\text{La}_2\text{CuO}_4$  are steeper at a higher temperature than at a lower, and seem to fall on identical curves at high temperatures. (3) The slope in the plot of the thermoelectric power,  $\alpha$ , vs.  $1/T$  decreases with an increase in the ionic radii of  $\text{Ln}^{3+}$ . The negative  $\alpha$  values of all the  $\text{Ln}_2\text{CuO}_4$  except for  $\text{La}_2\text{CuO}_4$  suggest that they are electron conductors. (4) The crystal structure of  $\text{Ln}_2\text{CuO}_4$  is tetragonal, and the lattice parameters,  $c$

8) T. Moeller, "The Chemistry of the Lanthanides," Reinhold Publishing Corporation, New York, N.Y. (1963), p. 21.

and  $a$ , of Ln, but not La, increase with an increase in the ionic radii of  $\text{Ln}^{3+}$ . The axis,  $a$ , of  $\text{La}_2\text{CuO}_4$ , however, becomes smaller than that of  $\text{Pr}_2\text{CuO}_4$  in spite of the fact that the ionic radius of  $\text{La}^{3+}$  is larger than that of  $\text{Pr}^{3+}$ , and its  $c$  axis expands more greatly than would be expected from the manner in the plots of  $c$  vs. the ionic radii of  $\text{Ln}^{3+}$  between Gd and Pr.

At this time it is hard to give a detailed explanation of the temperature dependence of resistivity shown in the summarized results (2), but we believe, as is generally thought for the same behavior of other semiconductors,<sup>9)</sup> that the less steep slopes in the lower-temperature region are mainly due to an extrinsic excitation process and that the steeper ones in the higher-temperature region are ascribable to an intrinsic process.

Measurements of the thermoelectric power, as is well known, provide information on carriers.<sup>10)</sup> The thermoelectric power,  $\alpha$ , is related to the dependence of the number of carriers,  $n$ , on the temperature,  $T$ , by the following equation:

$$\alpha = d\Delta\phi/dT = (kT/e)(d \log n/dT)$$

where  $\Delta\phi$  is the potential difference due to a temperature gradient given on a specimen rod,  $k$  is the Boltzmann constant, and  $e$  is the electronic charge. When the Maxwell distribution can be applied to  $d \log n/dT$ , or when:

$$n = N_0 \exp(-E/kT)$$

where  $E$  is the activation energy, and  $N_0$ , a constant, the following equation can be obtained:

$$\alpha = -E/Te.$$

This indicates that the slope in the plots of  $\alpha$  vs.  $1/T$  corresponds to the activation energy,  $E$ .<sup>10)</sup>

The negative thermoelectric power (shown in Fig. 4) indicates that the carriers in  $\text{Ln}_2\text{CuO}_4$  are electrons, supporting the extrinsic excitation procedure described in the previous paragraph, where it was not known whether the carriers were electrons or holes. The donor is most likely  $\text{Cu}^+$  formed by a partial decomposition of  $\text{Cu}^{2+}$  to  $\text{Cu}^+$ , because  $\text{Ln}_2\text{CuO}_4$  is decomposed to  $\text{Cu}_2\text{O}$  and  $\text{Ln}_2\text{O}_3$  at 1000–1200°C,<sup>11)</sup> although no significant amount of  $\text{Cu(I)}$  was found from the chemical analysis in this study.<sup>12)</sup>

A more detailed discussion of the electron configuration of  $\text{Cu}^{2+}$  is needed to explain the semiconductor-metal transition between  $\text{Pr}_2\text{CuO}_4$  and  $\text{La}_2\text{CuO}_4$  and the dependence of the activation energy on the ionic radii of  $\text{Ln}^{3+}$ . The valence electron configuration of  $\text{Cu}^{2+}$  is  $3d^9$ . As is shown in Fig. 6,  $\text{Cu}^{2+}$  is surrounded by six  $\text{O}^{2-}$  ions in the  $\text{Ln}_2\text{CuO}_4$ , so that the energy level of the 3d-electrons is split into several energy levels, depending upon the relative positions of the  $\text{O}^{2-}$  to  $\text{Cu}^{2+}$ . Now, the  $c$  axis is taken as  $z$ , and  $a$  is

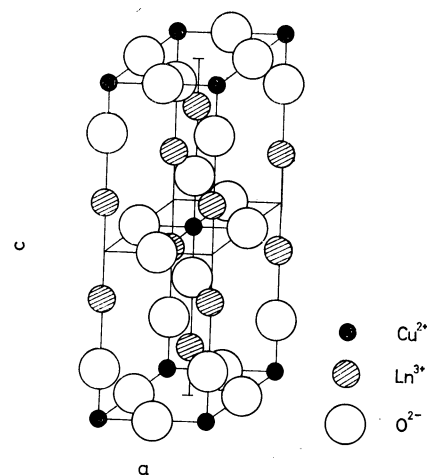


Fig. 6. Crystal structure of  $\text{Ln}_2\text{CuO}_4$

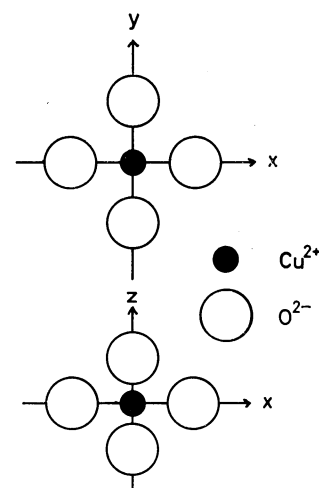


Fig. 7. Octahedron of  $\text{CuO}_6$

taken as an  $x$  or  $y$  coordinate; the  $\text{O}^{2-}$  are situated on  $x$  or  $y$ , as is illustrated in Fig. 7. The  $\text{O}^{2-}$  ion on  $x$  or  $y$  is not equivalent to that on  $z$ . It is not known yet which distance is longer,  $\text{Cu-O}$  on  $x$  (or  $y$ ) or  $\text{Cu-O}$  on  $z$ , but the similar  $c/a$  value of  $\text{K}_2\text{CuF}_4$  (3.066) to that of  $\text{Gd}_2\text{CuO}_4$  (3.046) suggests that the ratio of  $(\text{Cu-O})_x$  to  $(\text{Cu-O})_z$  for  $\text{Gd}_2\text{CuO}_4$  is essentially the same as that of  $(\text{Cu-F})_x$  to  $(\text{Cu-F})_z$  for  $\text{K}_2\text{CuF}_4$ ,  $(\text{Cu-F})_x = 2.078 \text{ \AA}$  and  $(\text{Cu-F})_z = 1.949 \text{ \AA}$ .<sup>3)</sup> Thus, we made an assumption, but one which is not essential in the following discussion, that  $(\text{Cu-O})_x$  is greater than  $(\text{Cu-O})_z$ . Since the energy level of the 3d-electrons of  $\text{Cu}^{2+}$  is split in such a way as to minimize the electrostatic energy due to a repulsive force between the electrons on the  $\text{Cu}^{2+}$  and  $\text{O}^{2-}$  anions, the most stable 3d-electron configuration of  $\text{Cu}^{2+}$  probably consists of four levels, as is illustrated in Fig. 8. The energy gaps among these four levels are affected by the ligand-field strength, which depends mainly upon the effective negative charge on  $\text{O}^{2-}$ . This effective charge on  $\text{O}^{2-}$  might be influenced by the size of  $\text{Ln}^{3+}$  in the manner that a more negative charge is provided by the larger (or lighter) rare earth cations, because the larger cations, which come from less electronegative rare earths, may

9) Stephan P. Mitoff, "Progress in Ceramic Science" Vol. 4 edited by J. E. Burke, Pergamon Press (1966), p. 217.

10) Takeo Kawaguchi, "Handotai no Kagaku" Maruzen Co., Ltd., (1971), p. 50.

11) M. Foex, A. Mancheron, and M. Line, *C. R. Acad. Sci. Paris*, **250**, 3027 (1960).

12) The content of the oxygen was obtained from the data of chemical analysis of Cu and Ln, and from the weight of the samples dissolved for the chemical analysis.

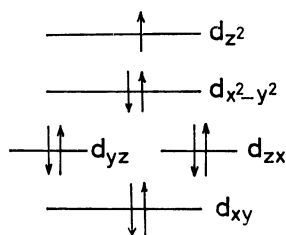


Fig. 8. 3d-electron configurations of  $\text{Cu}^{2+}$  in  $\text{Ln}_2\text{CuO}_4$   
( $\text{Ln}=\text{Gd}, \text{Sm}, \text{Nd}, \text{and Pr}$ )

well push electrons more strongly toward oxygen in the  $\text{Ln}-\text{O}$  bond. The greater effective charge, or the greater ligand-field strength, enhances the split energy gap of the 3d-electrons, so that, in the course of replacing the smaller rare earth cation with the larger one,  $e_g$  levels rise faster than do the  $t_{2g}$  levels, and so that in a rare-earth cation, at last, the  $e_g$  levels might be higher than the 4s or 4p level, with a slight structural modification, if necessary.

The trend shown in Figs. 2 and 5, the greater resistivity of the smaller  $\text{Ln}^{3+}$  compounds, can be explained as being due to: (1) more donors (probably  $\text{Cu}^+$ ) in the compounds of the larger rare earth cations and/or (2) the lower activation energy between the donor and the conduction level for the compounds of the larger rare earth cations. The temperature dependence of the resistivity alone (Fig. 2) does not clearly determine which factor predominates, because the slope in the  $\log \rho - 1/T$  plots is not so markedly dependent upon the rare earth of the  $\text{Ln}_2\text{CuO}_4$  and because the dependence of the mobility on the temperature may not be negligible, particularly for the sintered samples used in this study. The data of thermoelectric power shown in Fig. 4 suggest that the second case is more important; the slope in the plots of  $\alpha - 1/T$  increases with a decrease in the size of the rare earth cations. The excess electron on the  $\text{Cu}^+$  probably occupies the  $3d_{z^2}$ , donor level, which rises as the ligand field becomes stronger, so that the energy gap between the donor and the conduction level may be reduced, thus leading to the lower activation energy of the compounds of the larger rare earth cations.

The compound of the largest rare earth cation is  $\text{La}_2\text{CuO}_4$ . The shrinkage of the  $a$  axis and the expansion of the  $c$  axis compared to  $\text{Pr}_2\text{CuO}_4$  can be attributed to: (1) the depression of the electron density

in the  $x$  and  $y$  directions instead of the enhancement of that in the  $z$  direction and/or (2) a new chemical interaction or bonding between  $\text{Cu}^{2+}$  and  $\text{O}^{2-}$  in the  $x$  and  $y$  directions. Since the metallic conduction of  $\text{La}_2\text{CuO}_4$  surely suggests a new  $\pi$ -bond formation, because a  $\sigma$ -bond does not contribute to a metallic conduction, the second case described above must hold. The lowest energy level of electrons of  $\text{Cu}^{2+}$  which can make a  $\pi$ -bond with the 2p-electron of  $\text{O}^{2-}$  would be 4p, because: (1) the 3d levels except for  $e_g$  have already been filled, (2) electrons in the  $e_g$  levels are forbidden to make an overlapping with 2p in  $\text{O}^{2-}$  from the point of view of the symmetry, and (3) the 4s electron in  $\text{Cu}^{2+}$  can form only a  $\sigma$ -bond with 2p-electrons in  $\text{O}^{2-}$ . This new electron configuration is reasonable in view of the structural change observed between  $\text{Pr}_2\text{CuO}_4$  and  $\text{La}_2\text{CuO}_4$ .

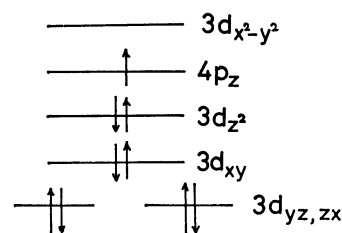


Fig. 9. Electron configuration of  $\text{Cu}^{2+}$  in  $\text{La}_2\text{CuO}_4$

The shrinkage of the  $a$  axis and the expansion of  $c$  axis enhance the electrostatic repulsive force between the  $\text{O}^{2-}$  anion and the  $3d_{x^2-y^2}$  electrons and reduce the same force between the  $\text{O}^{2-}$  anion and the  $3d_{z^2}$  electrons respectively. If the shrinkage of the  $a$  axis is great enough, the  $3d_{x^2-y^2}$  level would become higher than  $4p_z$  as well as  $3d_{z^2}$ .  $\text{La}_2\text{CuO}_4$  might be a case of this. If so, the above description leads to a similar electron configuration derived from the  $\pi$ -bond formation. Consequently, the most probable electron configuration is one electron in  $4p_z$ , two electrons in  $3d_{z^2}$ , and six electrons in  $t_{2g}$ , as is illustrated in Fig. 9. Thus,  $4p_z$  electrons in  $\text{Cu}^{2+}$  form a  $\pi$ -bond with  $2p_z$  electrons in  $\text{O}^{2-}$  over the  $\text{Cu}-\text{O}-\text{Cu}$  networks on the  $c$  planes, leading to a conduction band three quarters of which is filled with electrons. The conduction band described above also suggested by the magnetic properties of  $\text{La}_2\text{CuO}_4$ ; Pauli paramagnetism was observed for  $\text{La}_2\text{CuO}_4$ , suggesting collective electrons rather than localized ones.<sup>6)</sup>